

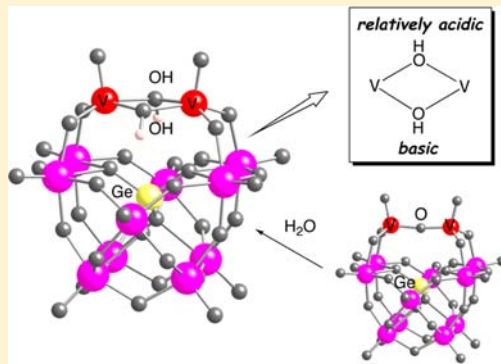
Effects of Isolobal Heteroatoms in Divanadium-Substituted γ -Keggin-type Polyoxometalates on $(\text{OV})_2(\mu\text{-OH})_2$ Diamond and $(\text{OV})_2(\mu\text{-O})$ Core Structures and the Transformation

Kazuhiro Uehara, Tatsuya Taketsugu, Kazuhiro Yonehara, and Noritaka Mizuno*

Department of Applied Chemistry, School of Engineering, The University of Tokyo, 7-3-1 Hongo, Bunkyo-ku, Tokyo 113-8656, Japan

Supporting Information

ABSTRACT: Effects of isolobal heteroatoms in divanadium-substituted γ -Keggin-type polyoxometalates, $(\text{TBA})_4[\gamma\text{-XV}_2\text{W}_{10}\text{O}_{38}(\mu\text{-OH})_2]$ 1^{X} and $(\text{TBA})_4[\gamma\text{-XV}_2\text{W}_{10}\text{O}_{38}(\mu\text{-O})]$ 2^{X} (where X = Ge or Si), on $(\text{OV})_2(\mu\text{-OH})_2$ and $(\text{OV})_2(\mu\text{-O})$ core structures and transformations from 2^{X} to 1^{X} have been investigated. X-ray crystallography of 1^{X} and 2^{X} reveals that larger Ge (covalent radius 1.22 Å; covalent radius of Si 1.11 Å) induces (a) expansion of $(\text{OV})_2(\mu\text{-OH})_2$ and $(\text{OV})_2(\mu\text{-O})$ cores, (b) expansion of lacunary sites, and (c) deep location of divanadium cores inside their lacunary sites. Density functional theory (DFT) calculations for anionic moieties of 1^{X} and 2^{X} reveal that energy levels of the highest occupied molecular orbital (HOMO)–1 in 1^{Ge} and HOMO in 2^{Ge} are lower than those in 1^{Si} and 2^{Si} , respectively, because of smaller contribution of p_z orbitals of oxygen atoms in 1^{Ge} and 2^{Ge} , which would result from shorter $\text{V}\cdots\text{O}(\text{-Ge})$ distances. Compound 2^{Ge} reacts with water vapor to form $(\text{TBA})_4[\gamma\text{-GeV}_2\text{W}_{10}\text{O}_{38}(\mu\text{-OH})_2]$ 1^{Ge} via a crystal-to-crystal transformation, and the water dissociation proceeds heterolytically. DFT calculations reveal that the reaction proceeds through (1) coordination of water on a coordinatively unsaturated site of vanadium in the lowest unoccupied molecular orbital (LUMO), followed by (2) proton transfer to the bridging oxo moiety. The order is different from that in 2^{Si} , which would result from the lower energy level of HOMO of 2^{Ge} (i.e., lower nucleophilicity toward a proton of water) than that of 2^{Si} .



INTRODUCTION

Bis(μ -hydroxo) or bis(μ -oxo)dimetal complexes with $\text{M}_2[\mu\text{-O}(\text{H})_2]$ diamond cores have extensively been studied since the 1990s, because these diamond core structures are frequently found as active centers in non-heme enzymes such as soluble methane monooxygenase, ribonucleotide reductase, tyrosinase, etc.¹ Therefore, analogous structures have been synthesized with a series of transition metals such as Mn, Fe, Co, Ni, Cu, Pd, etc., and their spectroscopic properties and reactivities toward various substrates have been investigated.^{2–7} Two hydroxyl groups in $\text{M}_2(\mu\text{-OH})_2$ cores generally act as bases, and their dehydrative condensation reactions with protic substrates such as alcohols, carboxylic acids, acetylene, and hydrogen peroxide proceed to afford the corresponding alkoxo, carboxylate, acetylido, and peroxy derivatives. In addition, a diamond core transformation from $\text{M}_2(\mu\text{-O})$ to $\text{M}_2(\mu\text{-OH})_2$ (where M = V, Mn, Fe, Co, etc.) has become a current research topics in coordination and bioinorganic chemistry.^{8–13} The reaction is also recognized as dissociation of water,^{14–17} which is quite difficult in the gas phase because of high Gibbs free energies (ΔG°) of 0.4934 and 1.635 $\text{MJ}\cdot\text{mol}^{-1}$ for homolysis and heterolysis, respectively.

Polyoxometalates (POMs) are nanosized anionic metal oxide clusters, consisting mainly of early transition metals and oxo moieties, that are frequently utilized as catalysts, magnetic

materials, pharmaceuticals, and building blocks of inorganic–organic hybrid materials.¹⁸ We have recently disclosed heterolytic dissociation of water on a (μ -oxo)divanadium(V)-substituted silicodecatungstate to form a bis(μ -hydroxo)-divanadium(V)-substituted silicodecatungstate via crystal-to-crystal transformation,¹³ suggesting that the two hydroxides in $\text{V}_2(\mu\text{-OH})_2$ behave in different ways.¹⁹ Because acidities, redox potentials, and energy levels of the lowest unoccupied molecular orbital (LUMO) and the highest occupied molecular orbital (HOMO) of POMs depend on the kinds of heteroatoms in POMs,^{20,21} investigation of the effects of heteroatoms on structures, chemical properties, and reactivities is interesting.

Here we report effects of isolobal heteroatoms in divanadium-substituted γ -Keggin type polyoxometalates, $(\text{TBA})_4[\gamma\text{-XV}_2\text{W}_{10}\text{O}_{38}(\mu\text{-OH})_2]$ 1^{X} and $(\text{TBA})_4[\gamma\text{-XV}_2\text{W}_{10}\text{O}_{38}(\mu\text{-O})]$ 2^{X} [where X = Ge (covalent radius 1.22 Å) or Si (1.11 Å); TBA = tetra(*n*-butyl)ammonium], on the $(\text{OV})_2(\mu\text{-OH})_2$ diamond and $(\text{OV})_2(\mu\text{-O})$ core structures and the transformation.

Received: November 16, 2012

Published: January 9, 2013



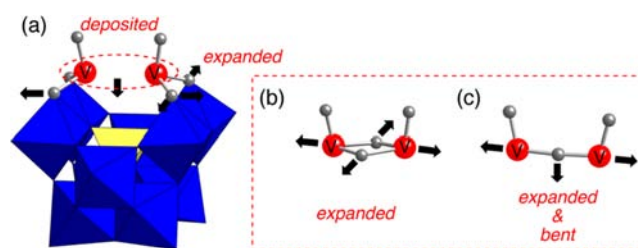
Table 1. Crystallographic Data for (TBA)₄[γ -GeV₂W₁₀O₃₈(μ -OH)₂] 1^{Ge} and 1'^{Ge} and (TBA)₄[γ -GeV₂W₁₀O₃₈(μ -O)] 2^{Ge}

	1 ^{Ge}	2 ^{Ge} ·(C ₂ H ₄ Cl ₂) ₂	1' ^{Ge} ·(C ₂ H ₄ Cl ₂)
empirical formula	C ₆₄ GeN ₄ O ₄₀ V ₂ W ₁₀	C ₆₈ Cl ₄ GeN ₄ O ₃₉ V ₂ W ₁₀	C ₆₆ Cl ₂ GeN ₄ O ₄₀ V ₂ W ₁₀
formula weight	3477.65	3651.49	3572.57
crystal system	monoclinic	tetragonal	tetragonal
lattice type	primitive	primitive	primitive
space group	P2 ₁ (no. 4)	P-421c (no. 114)	P-421c (no. 114)
lattice parameter <i>a</i> , Å	18.40680(10)	35.79400(10)	35.77260(10)
lattice parameter <i>b</i> , Å	14.48460(10)	35.79400(10)	35.77260(10)
lattice parameter <i>c</i> , Å	18.52710(10)	17.00030(10)	17.00200(10)
lattice parameter β , deg	94.41(0)		
lattice parameter <i>V</i> , Å ³	4924.99(5)	21780.96(15)	21757.10(15)
Z	2	8	8
<i>d</i> _{calc'd} , g·cm ⁻³	2.345	2.227	2.239
<i>F</i> ₀₀₀	3100	13 072	13 136
μ (Mo K α), mm ⁻¹	12.178	11.115	11.128
no. of reflns measd	13750	30114	31035
no. of observations	13582	29249	27519
no. of variables	299	469	341
<i>R</i> ₁ ^a	0.0299	0.0339	0.0403
<i>wR</i> ₂ ^a	0.1018	0.102	0.1183

^aData with *I* > 2.00 σ (*I*).

RESULTS AND DISCUSSION

Molecular Structures of Bis(μ -hydroxo)divanadium-Substituted γ -Keggin-type Germanodecatungstate (TBA)₄[γ -GeV₂W₁₀O₃₈(μ -OH)₂] 1^{Ge} and (μ -Oxo)-divanadium-Substituted γ -Keggin-type Germanodecatungstate (TBA)₄[γ -GeV₂W₁₀O₃₈(μ -O)] 2^{Ge}. Single crystals of 1^{Ge} and 2^{Ge} were successfully obtained, and these structures were determined by X-ray crystallography (Tables 1 and 2 and Figure 1). Compound 1^{Ge} crystallized in the monoclinic crystal system. Four TBA cations per an anionic moiety of 1^{Ge} were observed. The terminal V=O distances were 1.573(9) and 1.561(10) Å, respectively, suggesting a double-bond character. The V–O(–V) distances were in the range 1.975(8)–2.000(8) Å, and the bond valence sum (BVS) values of O(113) and O(114) were 1.19 and 1.24, respectively,²² indicating that bridging oxygen ligands between vanadium centers are assignable to hydroxides. The BVS values of V (5.02, 5.02), W (5.89–6.09), Ge (4.04), and O (1.53–2.11) indicate that the respective valences are +5, +6, +4, and –2 (Table S2, Supporting Information). The V...V distance was 3.168(3) Å, longer than that [3.096(4) Å] in 1^{Si}, showing expansion of the (OV)₂(μ -OH)₂ core in 1^{Ge} upon substitution of Si⁴⁺ with Ge⁴⁺. The O(115)...O(116) and O(117)...O(118) distances in 1^{Ge} were 5.26(1) and 5.29(1) Å, respectively, longer than those [5.19(2) and 5.22(2) Å] in 1^{Si}. On the other hand, the O(115)...O(118) and O(116)...O(117) distances in 1^{Ge} were 2.72(1) and 2.72(2) Å, respectively, very close to those [2.70(2) and 2.72(2) Å] in 1^{Si}. These facts also show expansion of the lacunary site in 1^{Ge} upon substitution of Si⁴⁺ with Ge⁴⁺. In addition, the Ge–O distances [1.715(6)–1.794(7) Å] in 1^{Ge} were longer than the Si–O ones [1.613(11)–1.633(12) Å] in 1^{Si}, while V...O(–Ge) distances [2.414(7) and 2.413(7) Å] in 1^{Ge} were shorter than V...O(–Si) ones [2.590(6) and 2.536(6) Å] in 1^{Si}. The Ge...V distances [3.705(3) and 3.725(3) Å] in 1^{Ge} were shorter than Si...V ones [3.755(5) and 3.737(5) Å] in 1^{Si}, showing that the (OV)₂(μ -OH)₂ core in 1^{Ge} is more deeply located inside the lacunary site. To date, divanadium complexes with a V₂(μ -OH)₂ diamond core are still rare from the viewpoint of coordination chemistry.^{23,24}

Table 2. Selected Bond Lengths and Angles for (TBA)₄[γ -GeV₂W₁₀O₃₈(μ -OH)₂] 1^{Ge} and 1'^{Ge} and (TBA)₄[γ -GeV₂W₁₀O₃₈(μ -O)] 2^{Ge}

	1 ^{Ge}	2 ^{Ge} ·(C ₂ H ₄ Cl ₂) ₂	1' ^{Ge} ·(C ₂ H ₄ Cl ₂)
V=O, Å	1.573(9), 1.561(10)	1.596(8), 1.606(8)	1.587(12), 1.593(10)
V–O(–V), Å	1.990(8), 1.981(8), 2.000(8), 1.975(8)	1.762(7), 1.771(7)	2.010(9), 2.043(9), 1.976(9), 2.000(9)
V–O(–W), Å	1.815(7), 1.814(8)	1.770(6), 1.748(6)	1.779(8), 1.809(7)
V...O(–Ge), Å	1.837(8), 1.816(7)	1.770(6), 1.783(6)	1.803(8), 1.838(3)
V...O(–Si), Å	2.414(7), 2.413(7)	2.591(6), 2.536(6)	2.425(8), 2.425(7)
Ge–O, Å	1.715(6), 1.730(6), 1.794(7), 1.744(6)	1.728(5), 1.738(6), 1.763(5), 1.756(5)	1.734(7), 1.745(6), 1.746(6), 1.746(6)
V...V, Å	3.168(3)	3.531(2)	3.226(3)
V–O–V, Å	105.1(4), 106.4(4)	176.2(5)	108.1(4), 105.9(4)
Ge...V, Å	3.705(3), 3.725(3)	3.918(2), 3.889(2)	3.751(3), 3.768(2)
O...O, Å	5.26(1), 5.29(1)	5.217(9), 5.172(9)	5.27(1), 5.28(1)
torsion angle, ^a deg	1.033	0.222	0.839

^aO(101)–V(101)...V(102)–O(102) angle.

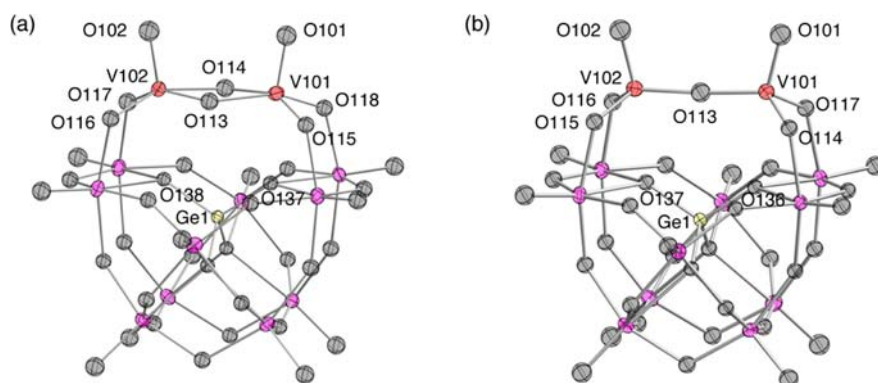


Figure 1. Thermal ellipsoid views of (a) $(\text{TBA})_4[\gamma\text{-GeV}_2\text{W}_{10}\text{O}_{38}(\mu\text{-OH})_2]$ 1^{Ge} and (b) $(\text{TBA})_4[\gamma\text{-GeV}_2\text{W}_{10}\text{O}_{38}(\mu\text{-O})]$ 2^{Ge} , drawn at 50% probability level (TBA cations were omitted for clarity).

Compound 2^{Ge} crystallized in the tetragonal crystal system. Four TBA cations per an anionic moiety of 2^{Ge} were also observed. The terminal $\text{V}=\text{O}$ distances were 1.596(8) and 1.606(8) Å, showing retention of the double-bond character. The BVS values of O (1.70–2.21), Ge (4.02), V (5.02 and 5.05), and W (5.89–6.11) indicate that the respective valences are -2 , $+4$, $+5$, and $+6$ (Table S3, Supporting Information). The BVS value of O(113) was 2.21, indicating that the bridging oxygen ligand between two vanadium centers is assignable to an oxo ligand. The $\text{V}\cdots\text{V}$ distance was 3.531(2) Å, longer than that [3.505(4) Å] in 2^{Si} , showing expansion of the $(\text{OV})_2(\mu\text{-O})$ core in 2^{X} upon substitution of Si^{4+} with Ge^{4+} . The $\text{O}(115)\cdots\text{O}(116)$ and $\text{O}(117)\cdots\text{O}(118)$ distances in 2^{Ge} were 5.217(9) and 5.172(9) Å, respectively, longer than those [5.05(2) and 5.12(2) Å] in 2^{Si} . In addition, the $\text{O}(115)\cdots\text{O}(118)$ and $\text{O}(116)\cdots\text{O}(117)$ distances in 2^{Ge} were 2.825(9) and 2.81(1) Å, respectively, longer than those [2.79(2) and 2.77(2) Å] in 2^{Si} . These facts also show expansion of the lacunary site in 2^{X} upon substitution of Si^{4+} with Ge^{4+} . In addition, the $\text{Ge}-\text{O}$ distances [1.728(5)–1.763(5) Å] in 2^{Ge} were longer than the $\text{Si}-\text{O}$ ones [1.624(9)–1.650(9) Å] in 2^{Si} , while $\text{V}\cdots\text{O}(-\text{Ge})$ distances [2.591(6) and 2.536(6) Å] in 2^{Ge} were shorter than $\text{V}\cdots\text{O}(-\text{Si})$ ones [2.706(8) and 2.760(8) Å] in 2^{Si} . The $\text{Ge}\cdots\text{V}$ distances [3.918(2) and 3.889(2) Å] in 2^{Ge} were shorter than the $\text{Si}\cdots\text{V}$ ones [3.965(4) and 4.005(4) Å] in 2^{Si} , showing that the $(\text{OV})_2(\mu\text{-O})$ core in 2^{Ge} is more deeply located inside the lacunary site. The $\text{V}-\text{O}-\text{V}$ angle and the torsion angle between $\text{O}(101)-\text{V}(101)$ and $\text{V}(102)-\text{O}(102)$ in 2^{Ge} were $176.2(5)^\circ$ and 0.222° , respectively, showing syn-angular conformation of the $(\text{OV})_2(\mu\text{-O})$ core.^{13,25–29} All these results show that the lacunary sites in 1^{X} and 2^{X} are expanded and the divanadium cores are more deeply located inside the lacunary sites upon substitution of Si^{4+} with the larger Ge^{4+} .

Density Functional Theory Calculations of Anionic Parts of $(\text{TBA})_4[\gamma\text{-XV}_2\text{W}_{10}\text{O}_{38}(\mu\text{-OH})_2]$ 1^{X} and $(\text{TBA})_4[\gamma\text{-XV}_2\text{W}_{10}\text{O}_{38}(\mu\text{-O})]$ 2^{X} ($\text{X} = \text{Ge}, \text{Si}$).^{29–31} Selected molecular orbitals of 1^{X} are shown in Figures 2 and S8 (Supporting Information). The energy levels of LUMO of 1^{Ge} and 1^{Si} were -3.442 and -3.448 eV, respectively, very close to each other. The energy levels of HOMO of 1^{Ge} and 1^{Si} were -7.508 and -7.512 eV, respectively, also very close to each other. The coefficients of p_z orbitals of O(137) and O(138) in LUMO of 1^{Ge} were 0.00000 and 0.00000, respectively, and those in HOMO were 0.00000 and 0.00000, respectively. Similarly, coefficients of p_z orbitals of O(137) and O(138) in LUMO of

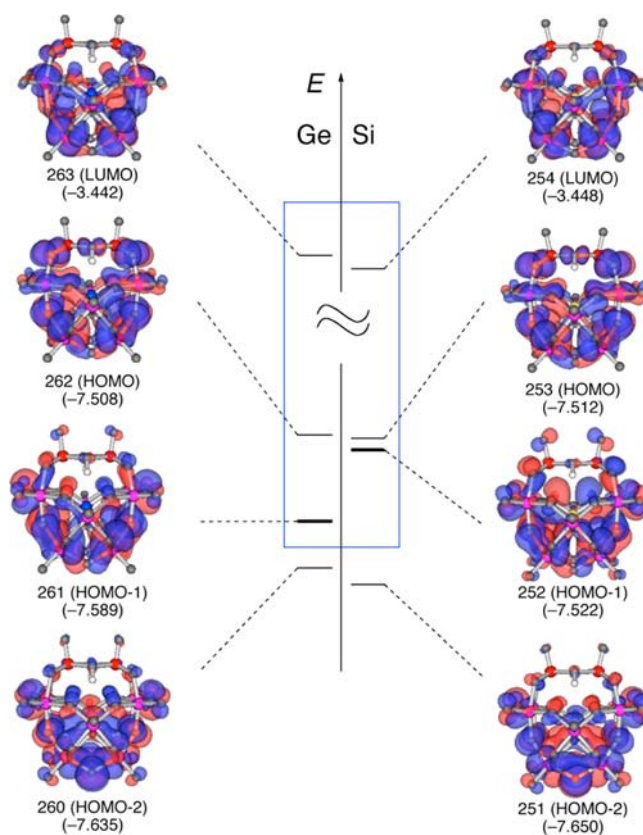


Figure 2. Energy diagrams of $(\text{TBA})_4[\gamma\text{-XV}_2\text{W}_{10}\text{O}_{38}(\mu\text{-OH})_2]$ 1^{X} under water ($\text{X} = \text{Ge}$ or Si ; isosurface value 0.015; energies in parentheses are in electronvolts; blue, positive phase, and red, negative phase).

1^{Si} were 0.00005 and 0.00003, respectively, and those in HOMO were -0.01430 and -0.00114 , respectively. Therefore, p_z orbitals of O(137) and O(138) did not contribute to LUMO and HOMO of 1^{X} .

On the other hand, the energy levels of HOMO–1 of 1^{Ge} and 1^{Si} were -7.589 and -7.522 eV, respectively, and the energy level of 1^{Ge} was lower than that of 1^{Si} . The coefficients of p_z orbitals of O(137) and O(138) in HOMO–1 of 1^{Ge} were -0.07129 and 0.07129 , respectively, and these p_z orbitals did not contribute much to HOMO–1. On the other hand, the coefficients of p_z orbitals of O(137) and O(138) of 1^{Si} were 0.210 and -0.210 , respectively, and these p_z orbitals contributed most to HOMO–1. The shorter $\text{V}\cdots\text{O}(-\text{Ge})$

distances [stronger interaction between V and O(−Ge)] in 1^{Ge} than those in 1^{Si} would lead to smaller contribution of p_z orbitals of O(137) and O(138) to HOMO−1 of 1^{Ge} and a lower energy level of HOMO−1 of 1^{Ge} than that of 1^{Si} .

Selected molecular orbitals for 2^{X} are shown in Figures 3 and S5 (Supporting Information). The energy levels of HOMO

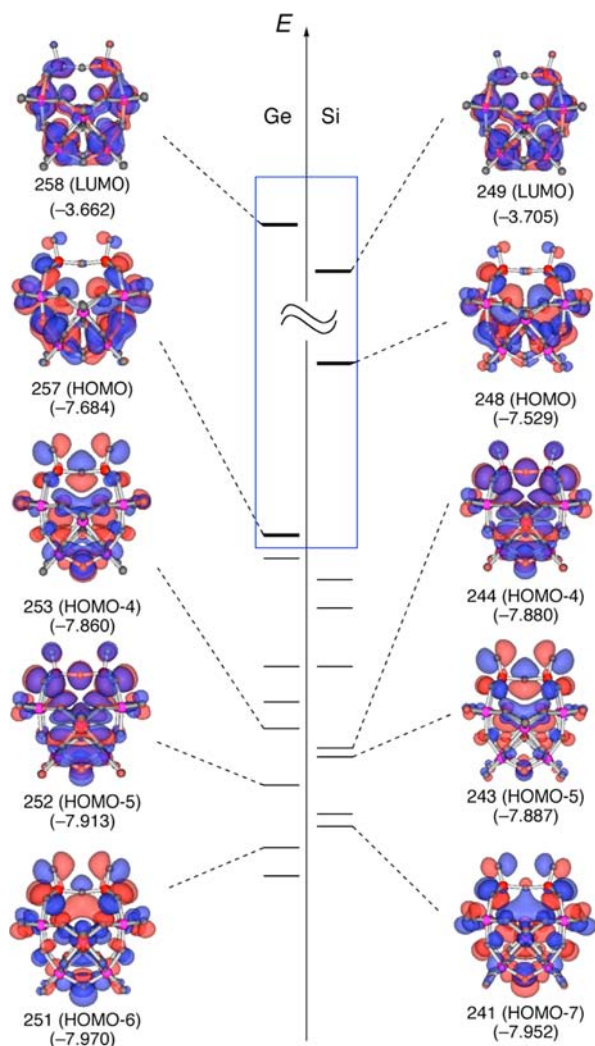


Figure 3. Energy diagrams of $(\text{TBA})_4[\gamma\text{-XV}_2\text{W}_{10}\text{O}_{38}(\mu\text{-O})] 2^{\text{X}}$ under water ($\text{X} = \text{Ge}$ or Si ; isosurface value 0.015; energies in parentheses are in electronvolts; blue, positive phase, and red, negative phase).

2^{Ge} and 2^{Si} were -7.684 and -7.529 eV, respectively, and the energy level of 2^{Ge} was much lower than that of 2^{Si} . The coefficients of p_z orbitals of O(136) and O(137) in HOMO of 2^{Ge} were 0.12875 and -0.12875 , respectively, while those of 2^{Si} were 0.26801 and -0.26801 , respectively, and these p_z orbitals contributed most to HOMO. The shorter $\text{V}\cdots\text{O}(\text{-Ge})$ distances [stronger interaction between V and O(−Ge)] in 2^{Ge} would lead to smaller contribution of p_z orbitals of O(136) and O(137) to HOMO of 2^{Ge} and a lower energy level of HOMO of 2^{Ge} than that of 2^{Si} [lower nucleophilicity on O(113)]. On the other hand, the energy levels of LUMO of 2^{Ge} and 2^{Si} , which include orbitals of coordinatively unsaturated sites on the divanadium center, were -3.662 and -3.705 eV, respectively, and the energy level of LUMO of 2^{Ge} was a little higher than that of 2^{Si} , suggesting the closer electrophilicity on the vanadium center of 2^{Ge} to that of 2^{Si} . Thus, the energy

levels of HOMO−1 in 1^{X} and HOMO and LUMO in 2^{X} are influenced by substitution of Si^{4+} with Ge^{4+} .³²

Crystal-to-Crystal Transformation from $(\text{TBA})_4[\gamma\text{-GeV}_2\text{W}_{10}\text{O}_{38}(\mu\text{-O})] 2^{\text{Ge}}$ to $(\text{TBA})_4[\gamma\text{-GeV}_2\text{W}_{10}\text{O}_{38}(\mu\text{-OH})_2] 1'^{\text{Ge}}$ and the Reaction Mechanism. When a dark red crystal of 2^{Ge} was placed under a humid atmosphere for 3 min, its crystal color changed to orange (Figure 4a). After successive treatment with water vapor for 6 h, the crystal color completely changed to yellow. The molecular structure was successfully determined by X-ray crystallography (Tables 1 and 2 and Figure 4b). Four TBA cations per anion were found in $1'^{\text{Ge}}$. The BVS values of O(113) and O(114) were 1.20 and 1.11, respectively, suggesting that these oxygen atoms are assignable to hydroxo ligands. The BVS values of V (4.86, 4.96), W (5.95–6.10), Ge (4.06), and the other oxygen atoms (1.68–2.06) suggest that the respective valences in $1'^{\text{Ge}}$ are +5, +6, +4, and -2 . These data reveal formation of a bis(μ -hydroxo)-divanadium-substituted polyoxometalate $(\text{TBA})_4[\gamma\text{-GeV}_2\text{W}_{10}\text{O}_{38}(\mu\text{-OH})_2]$ by crystal-to-crystal transformation as that from 2^{Si} to 1^{Si} . The V...V distance in $1'^{\text{Ge}}$ was $3.226(3)$ Å, shorter than that in 2^{Ge} and a little longer than that in 1^{Ge} , while the V=O [$1.587(12)$ and $1.593(10)$ Å], V−O(−V) [$1.976(9)$ – $2.043(9)$ Å], and V...O(−Ge) [$2.425(8)$ and $2.425(7)$ Å] distances in $1'^{\text{Ge}}$ were close to those [$1.573(9)$ and $1.561(10)$ Å; $1.975(8)$ – $2.000(8)$ Å; $2.414(7)$ and $2.413(7)$ Å, respectively] in 1^{Ge} . Accordingly, compound $1'^{\text{Ge}}$ would be recognized as an intermediate between 2^{Ge} and 1^{Ge} .

Figure 4c,d depicts crystal packings of 2^{Ge} and $1'^{\text{Ge}}$, respectively, along the c axis. Three kinds of channels (A–C) with diameters of approximately 2.76, 2.87, and 2.36 Å were observed in both 2^{Ge} and $1'^{\text{Ge}}$ and accommodated 1,2-dichloroethane solvents of crystallization. During transformation, water vapor (diameter approximately 1.78 Å) would diffuse into the channel and approach the $(\text{OV})_2(\mu\text{-O})$ core in 2^{Ge} .

The energy diagram of the water dissociation reaction with 2^{Ge} is shown in Figure 5. The coordination of water to the vanadium center via LUMO led to formation of TS^{Ge} . Successive proton transfer to the bridging oxo ligand resulted in formation of 1^{Ge} . The valence of the vanadium did not change in each step. The calculated activation and formation energies were 88.62 and -33.73 $\text{kJ}\cdot\text{mol}^{-1}$, respectively. Thus, the water dissociation reaction on 2^{Ge} proceeded heterolytically in a different way from that of 2^{Si} (proton transfer to the bridging oxo ligand followed by coordination of water to the vanadium center; TS^{Si} in Figure 5), as has been described in our previous report.¹³ This difference would result from the lower energy level of HOMO (i.e., lower nucleophilicity toward a proton of water) of 2^{Ge} and the close energy level of LUMO of 2^{Ge} to that of 2^{Si} . Such a diamond core interconversion might play a pivotal role in the various enzymatic reactions related to non-heme enzymes. The present results would give new insight into the reactivities of $\text{M}_2(\mu\text{-OH})_2$ diamond cores in transition-metal complexes.

Acidity of $[\gamma\text{-XV}_2\text{W}_{10}\text{O}_{38}(\mu\text{-OH})_2]^{4-}$. ^1H NMR signals of OH groups for 1^{Ge} and 1^{Si} were observed at 5.02 and 4.99 ppm, respectively. These OH groups of 1^{X} were placed in almost equivalent circumstances and exhibited almost the same basicity. In addition, the acidity of 1^{X} was estimated with ΔG° values of two deprotonation steps $\{\Delta G^\circ(1), [\gamma\text{-XV}_2\text{W}_{10}\text{O}_{38}(\mu\text{-OH})_2]^{4-} 1^{\text{X}} \rightarrow [\gamma\text{-XV}_2\text{W}_{10}\text{O}_{38}(\mu\text{-OH})(\mu\text{-O})]^{5-} \text{A}^{\text{X}}, \text{ and } \Delta G^\circ(2), [\gamma\text{-XV}_2\text{W}_{10}\text{O}_{38}(\mu\text{-OH})(\mu\text{-O})]^{5-} \text{A}^{\text{X}} \rightarrow [\gamma\text{-XV}_2\text{W}_{10}\text{O}_{38}(\mu\text{-O})_2]^{6-} \text{B}^{\text{X}}\}$ in water calculated by DFT. The

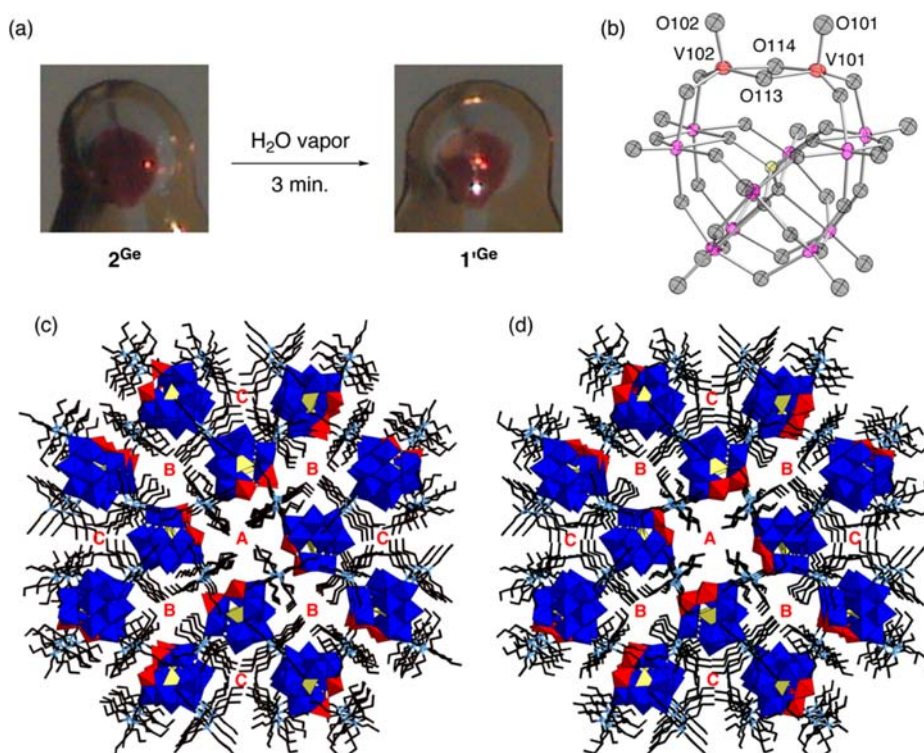


Figure 4. Crystal-to-crystal transformation from 2^{Ge} to $1'^{\text{Ge}}$. (a) Single crystals of 2^{Ge} and 2^{Ge} upon treatment with water vapor ($1'^{\text{Ge}}$). (b) Thermal ellipsoid plot of $1'^{\text{Ge}}$ drawn at 50% probability level (TBA cations and solvents of crystallization were omitted for clarity). (c, d) Crystal packing of (c) 2^{Ge} and (d) $1'^{\text{Ge}}$ along c -axis (A–C represent putative pathways for diffusion of water vapor).

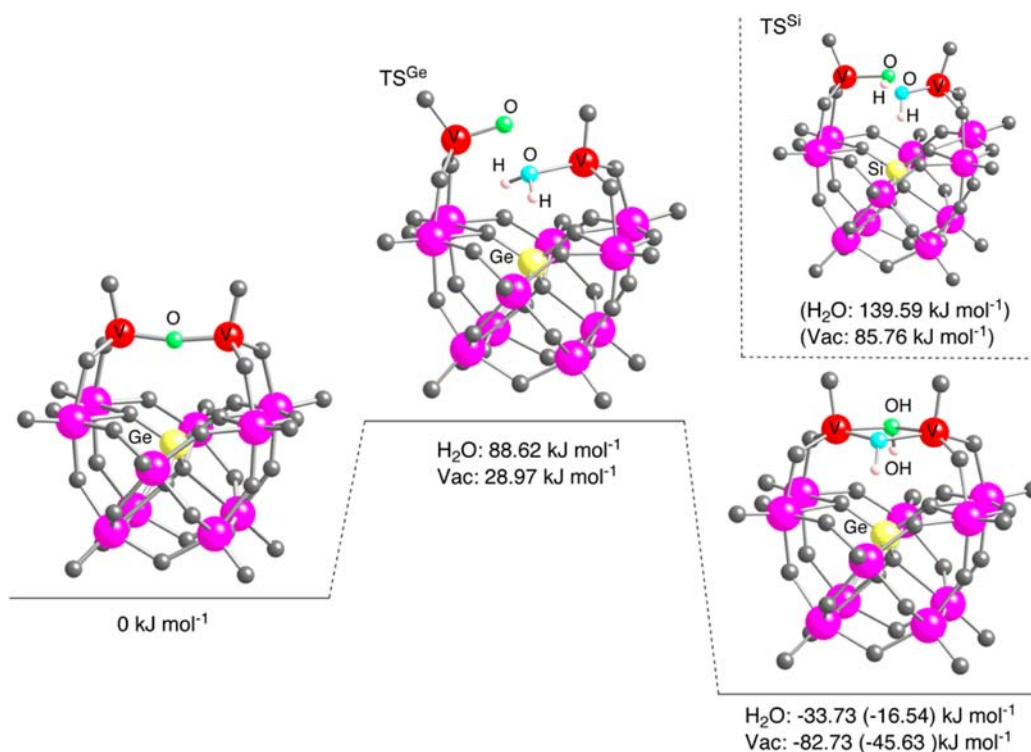
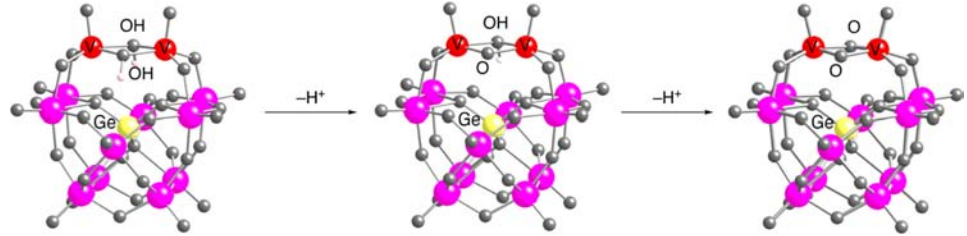


Figure 5. Energy diagram for heterolytic dissociation of water with $(\text{TBA})_4[\gamma\text{-GeV}_2\text{W}_{10}\text{O}_{38}(\mu\text{-O})] 2^{\text{Ge}}$ (energy in parentheses is that for Si derivatives).

results are summarized in Table 3. The $\Delta G^\circ(1)$ values for the deprotonations from 1^{Si} to A^{Si} and from 1^{Ge} to A^{Ge} in water were calculated to be $86.27 \text{ kJ}\cdot\text{mol}^{-1}$ [$\text{p}K_{\text{a}}(1) = 15.12$] and $93.67 \text{ kJ}\cdot\text{mol}^{-1}$ [$\text{p}K_{\text{a}}(1) = 16.42$], respectively. The $\Delta G^\circ(2)$

values for the successive deprotonation from A^{Si} into B^{Si} and from A^{Ge} into B^{Ge} were calculated to be $126.68 \text{ kJ}\cdot\text{mol}^{-1}$ [$\text{p}K_{\text{a}}(2) = 22.19$] and $122.81 \text{ kJ}\cdot\text{mol}^{-1}$ [$\text{p}K_{\text{a}}(2) = 21.52$], respectively. Therefore, the acidity of the two protons in 1^{X} is

Table 3. Acidity of $[\gamma\text{-H}_2\text{XV}_2\text{W}_{10}\text{O}_{40}]^{4-}$ (X = Si or Ge) in Water by DFT Calculations^a


X	$V_2(\mu\text{-OH})_2$ 1^X , hartree	$V_2(\mu\text{-OH})(\mu\text{-O})$ A^X , hartree	$V_2(\mu\text{-O})_2$ B^X , hartree	$\Delta G^\circ(1)$, ^b kJ·mol ⁻¹	$\Delta G^\circ(2)$, ^b kJ·mol ⁻¹	pK _a (1) ^c	pK _a (2) ^c
Si	-4125.00685413	-4124.55025899	-4124.07826913	86.27	126.68	15.12	22.19
Ge	-5910.49846930	-5910.03905243	-5909.56853687	93.67	122.81	16.42	21.52

^aGeometry optimization in water was carried out with 6-31G*/LanL2DZ hybrid basis set at the B3LYP level of theory. Single-point energy calculation in water was carried out with 6-311++G**/LanL2DZ hybrid basis set at the B3LYP level of theory. ^b $\Delta G^{\text{sol}}(\text{H}_3\text{O}^+) = -265.9$ kcal·mol⁻¹, reported in ref 33. ^cpK_a = (log₁₀ e)($\Delta G^\circ/RT$).

estimated to be close to those in 1^{Si} (Table S1, Supporting Information), which is consistent with results of ¹H NMR signals of OH groups. These results lead to the conclusion that (i) the isolobal heteroatom in the same group does not so much affect the acidity of POM and (ii) the differences of acidity for two hydroxyl groups of 1^X probably play an important role in the water dissociation reaction on 2^X .

CONCLUSION

X-ray crystallography of 1^X and 2^X reveals that larger Ge induces (a) expansion of $(\text{OV})_2(\mu\text{-OH})_2$ and $(\text{OV})_2(\mu\text{-O})$ cores, (b) expansion of lacunary sites, and (c) deep location of divanadium cores inside the lacunary sites. DFT calculations reveal that larger Ge also induces lower energy levels of HOMO-1 in 1^{Ge} and HOMO in 2^{Ge} , because of smaller contribution of p_z orbitals of oxygen atoms between V and Ge, which would result from longer V...O(-Si) distances. Heterolytic dissociation of water was demonstrated by a crystal-to-crystal transformation from 2^{Ge} to 1^{Ge} in the same way as that from 2^{Si} to 1^{Si} . DFT calculations reveal that the reaction with 2^{Ge} proceeds through (1) coordination of water on coordinatively unsaturated vanadium center via LUMO, followed by (2) proton transfer to the bridging oxo moiety. The order is different from that in 2^{Si} , which would result from the lower energy level of HOMO of 2^{Ge} (i.e., lower nucleophilicity toward a proton of water) than that of 2^{Si} .

EXPERIMENTAL SECTION

General Procedures. Manipulations were carried out under aerobic conditions except for the synthesis of $(\text{TBA})_4[\gamma\text{-GeV}_2\text{W}_{10}\text{O}_{38}(\mu\text{-O})] 2^{\text{Ge}}$. Solvents such as 1,2-dichloroethane, diethyl ether (Et₂O), and acetonitrile-*d*₃ (CD₃CN) were used as purchased. Compound $\text{K}_8[\gamma\text{-GeW}_{10}\text{O}_{36}]$ was synthesized according to the literature.³⁴ ¹H (500 MHz), ¹³C{¹H} (124.50 MHz), ⁵¹V{¹H} (130.23 MHz), and ⁵¹V MAS (130.23 MHz) NMR spectra were recorded on a JEOL ECA-500 spectrometer. Infrared spectra were recorded on a Jasco Fourier transform infrared (FT-IR) 580 spectrometer. Cold-spray ionization mass spectrometry (CSI-MS) spectra were measured with a JEOL T100-CS instrument.

Synthesis of $(\text{TBA})_4[\gamma\text{-GeV}_2\text{W}_{10}\text{O}_{38}(\mu\text{-OH})_2] 1^{\text{Ge}}$. A potassium salt of a dilacunary γ -germanodectungstate $\text{K}_8[\gamma\text{-GeW}_{10}\text{O}_{36}] \cdot 6\text{H}_2\text{O}$ (21.0 g, 7.22 mmol) was dissolved in 73.5 mL of 1 M HCl. The solution was cooled to 273 K with an ice bath, followed by addition of 75 mL of aqueous solution of NaVO₃ (1.76 g, 14.4 mmol). The resulting solution was stirred for 5 min, the solution was filtered to remove insoluble materials, and RbCl (10.5 g, 86.8 mmol) was added to give yellow precipitates. Washing with 5 mL of water gave yellow

powders of $\text{Rb}_2\text{K}_2[\gamma\text{-GeV}_2\text{W}_{10}\text{O}_{38}(\mu\text{-OH})_2]$ (1.90 g, 0.64 mmol) in 8.9% yield. The resultant $\text{Rb}_2\text{K}_2[\gamma\text{-GeV}_2\text{W}_{10}\text{O}_{38}(\mu\text{-OH})_2]$ was dissolved in 120 mL of 0.05 M HCl, and tetra(*n*-butyl)ammonium bromide (1.75 g, 5.4 mmol) was added into the solution to give pale yellow precipitates. The precipitates were dissolved in 15 mL of acetonitrile, and the solution was slowly added into 1 L of water. Filtration gave the pale yellow powder of $(\text{TBA})_4[\gamma\text{-GeV}_2\text{W}_{10}\text{O}_{38}(\mu\text{-OH})_2] 1^{\text{Ge}}$ (1.30 g, 0.35 mmol) in 54% yield. IR (KBr) (cm⁻¹) 3493 m [$\nu(\text{O-H})$], 2962 m, 2934 m, 2873 m [$\nu(\text{C-H})$], 1483 m [$\nu(\text{N-H})$], 1380 m, 1172 w, 1106 w, 1107 w, 1002 m, 964 s [$\nu(\text{V=O})$], 876 s, 854 s, 811 w, 761 s, 679 m, 541 m, 462 m, 395 m, 373 m, 348 m, 279 w. ¹H NMR (500 MHz, CD₃CN, room temperature, rt) δ_{H} (parts per million, ppm) 5.02 (br s, 2H, OH), 3.16 (t, ²J = 7.15 Hz, 32H, NCH₂), 1.64 (quint, ²J = 7.7 Hz, 32H, CH₂), 1.40 (sextet, ²J = 7.45 Hz, 32H, CH₂), 0.99 (t, ²J = 7.4 Hz, 48H, CH₃). ¹³C{¹H} NMR (124.5 MHz, CD₃CN, rt) δ_{C} (ppm) 59.24 (NCH₂), 24.33 (CH₂), 20.31 (CH₂), 13.85 (Me). ⁵¹V{¹H} NMR δ_{V} (ppm) -546.28. CSI-MS (263 K, CH₃CN) *m/z* 3866.96 (centered at *m/z* 3867.20, calculated for $\{(\text{TBA})_5[\text{H}_2\text{GeV}_2\text{W}_{10}\text{O}_{40}]^+\}$). Anal. calcd for C₆₄H₁₄₄N₄GeV₂W₁₀O₄₀: C, 21.21; H, 4.06; N, 1.55. Found: C, 20.94; H, 3.74; N, 1.51.

Synthesis of $(\text{TBA})_4[\gamma\text{-GeV}_2\text{W}_{10}\text{O}_{38}(\mu\text{-O})] 2^{\text{Ge}}$. Compound 1 (0.300 g, 82.8 μmol) was dissolved in dehydrated 1,2-dichloroethane (10 mL), followed by addition of PhNCO (1.0 g, 8.39 mmol). Keeping the reaction solution for 2 days gave dark red crystals of 3 (0.132 g, 36.6 μmol) in 45% yield. IR (KBr) (cm⁻¹) 3490 m [$\nu(\text{O-H})$], 2961 s, 2933 m, 2872 m [$\nu(\text{C-H})$], 1701 w, 1622 w, 1593 w, 1530 w, 1483 s, 1381 m [$\nu(\text{C-N})$], 1150 s, 1002 m, 964 vs, 876 vs, 854 vs, 836 vs, 811 vs, 762 vs, 677 m, 540 w, 462 m, 445 m, 394 m, 372 m, 347 m, 338 m, 279 m. ⁵¹V MAS NMR (130.23 MHz, rt) δ_{V} (ppm) -566.9. Anal. calcd for C₆₄H₁₄₄N₄GeV₂W₁₀O₃₉: C, 21.31; H, 4.02; N, 1.55. Found: C, 21.27; H, 3.85; N, 1.59.

Crystal-to-Crystal Transformation from 2^{Ge} to 1^{Ge} . A single crystal of 2^{Ge} was placed in a humid atmosphere for 3 min. The single-crystal X-ray measurement was carried out again, and the molecular structure of $(\text{TBA})_4[\gamma\text{-GeV}_2\text{W}_{10}\text{O}_{38}(\mu\text{-OH})_2] 1^{\text{Ge}}$ was determined. Similarly, dark red crystals of 2^{Ge} in the open bottle were placed in a screw bottle containing water for 3 min. Pale orange powders of 1^{Ge} were obtained in a quantitative yield. IR (KBr) (cm⁻¹) 3490 m [$\nu(\text{O-H})$], 2961 m, 2933 m, 2872 m [$\nu(\text{C-H})$], 1699 w, 1621 w, 1595 w, 1535 w, 1483 m [$\nu(\text{C-N})$], 1381 m, 1312 w, 1228 w, 1152 w, 1106 w, 1064 w, 1002 m, 964 s, 876 s, 854 s, 811 vs, 762 s, 677 m, 540 m, 462 m, 445 m, 540 m, 462 m, 445 m, 394 m, 372 m, 347 m, 338 m, 320 s, 310 s, 302 w, 279 m. ⁵¹V MAS NMR (130.23 MHz) δ_{V} -543.2 ppm. CSI-MS (263 K, CH₃CN) *m/z* 3867.04 (centered at *m/z* 3867.20, calculated for $\{(\text{TBA})_5[\text{H}_2\text{GeV}_2\text{W}_{10}\text{O}_{40}]^+\}$). Anal. calcd for C₆₄H₁₄₄N₄GeV₂W₁₀O₄₀: C, 21.21; H, 4.06; N, 1.55. Found: C, 21.42; H, 3.99; N, 1.54.

Details of X-ray Crystallography. Diffraction measurements were made on a Rigaku MicroMax-007 instrument with Mo K α radiation ($\lambda = 0.710$ 69 Å). Data collections were carried out at 153 K. Indexing was performed from 12 oscillation images, which were

exposed for 5 s. The crystal-to-detector distance was 45 mm. Readout was performed with pixel size 72.4×72.4 mm. A sweep of data was done with ω scans from -110° to 70° at $\kappa = 45^\circ$ and $\phi = 0^\circ, 90^\circ$. A total of 720 images for each compound were collected. Neutral scattering factors were obtained from the standard source.³⁵ Data were corrected for Lorentz and polarization effects. Empirical absorption corrections were made with HKL 2000 for Linux.³⁶ Molecular structures were solved by SHELX-97³⁷ linked to Win-GX for Windows.³⁸ More detailed descriptions about X-ray crystallography are given in the Supporting Information. CCDC files 908040 (1^{Ge}), 908038 ($1'^{\text{Ge}}$), and 908039 (2^{Ge}) contain the supplementary crystallographic data. The data can be obtained free of charge via www.ccdc.cam.ac.uk/conts/retrieving.html (or from the Cambridge Crystallographic Data Centre, 12 Union Rd., Cambridge CB2 1EZ, U.K.; fax (+44) 1223-336-033 or deposit@ccdc.cam.ac.uk).

Details of DFT Calculations. DFT calculations were performed with Gaussian09 software. Anionic parts of 1^{Ge} , 2^{Ge} , the transition states (TS^{Ge}), and the deprotonated 1^{X} (A^{X} and B^{X} ; X = Ge or Si) were optimized by use of 6-31G*/LanL2DZ or 6-31G* (6D,7F) at the B3LYP level of theory. Frequency calculations for TS^{Ge} were also carried out at the same level of theory. The corresponding single-point energy calculations for anionic parts of 1^{Ge} , 2^{Ge} , and the transition states (TS^{Ge}) were carried out with 6-311++G** (for O and H)/6-31G* (for Ge)/LanL2DZ (for V and W) at the B3LYP level of theory. Similarly, with the solvation in water taken into account, DFT calculations using the conductorlike polarizable continuum model (IEFPCM) with the parameter sets of United Atom Topological Model (UAKE) were carried out. Frequency calculations were also carried out at the same level of theory. The zero potential energy (ZPE) was not considered in evaluation of the energy.

■ ASSOCIATED CONTENT

Supporting Information

Additional text, four tables, and 16 figures giving crystallographic data for 1^{Ge} , $1'^{\text{Ge}}$, and 2^{Ge} and details of crystallography and DFT calculations; and complete ref 29. This material is available free of charge via the Internet at <http://pubs.acs.org>.

■ AUTHOR INFORMATION

Corresponding Author

*E-mail: tmizuno@mail.ecc.u-tokyo.ac.jp. Phone: +81-3-5841-7272. Fax: +81-3-5841-7220.

Notes

The authors declare no competing financial interest.

■ ACKNOWLEDGMENTS

This work was supported by Japan and Grants-in-Aid for Scientific Research, Ministry of Education, Culture, Science, Sports and Technology of Japan (MEXT) and Japan, and Funding Program for World-Leading Innovative R&D on Science and Technology (FIRST Program) of the Japan Society for the Promotion of Science (JSPS).

■ REFERENCES

- (1) (a) Thematic issues on biomimetic inorganic chemistry: Holm, R. H.; Solomon, E. I., Eds. *Chem. Rev.* **2004**, *104*, 347–1200. (b) *Activation of Small Molecules*; Tolman, W. B., Ed.; Wiley-VCH: Weinheim, Germany, 2006. (c) Que, L., Jr.; Tolman, W. B. *Angew. Chem., Int. Ed.* **2002**, *41*, 1114–1137. (d) Friedle, S.; Reisner, E.; Lippard, S. J. *Chem. Soc. Rev.* **2010**, *39*, 2768–2779. (e) Kitajima, N.; Tolman, W. B. *Adv. Inorg. Chem.* **1995**, *43*, 419–531. (f) Ito, S.; Fukuzumi, S. *Acc. Chem. Res.* **2007**, *40*, 592–600. (g) Akita, M.; Hikichi, S. *Bull. Chem. Soc. Jpn.* **2002**, *75*, 1657–1679. (h) Suzuki, M. *Acc. Chem. Res.* **2007**, *40*, 603–617. (i) Gilje, J. W.; Roesky, H. W. *Chem. Rev.* **1994**, *94*, 895–910.
- (2) (a) Wikstrom, J. P.; Filatov, A. S.; Mikhalyova, E. A.; Shatruck, M.; Foxman, B. M.; Rybak-Akimova, E. V. *Dalton Trans.* **2010**, *39*, 2504–2514. (b) Manzur, J.; Vega, A.; García, A. M.; Acuña, C.; Sieger, M.; Sarkar, B.; Niemeyer, M.; Lissner, F.; Schleid, T.; Kaim, W. *Eur. J. Inorg. Chem.* **2007**, 5500–5510.
- (3) Itoh, K.; Hayashi, H.; Furutachi, H.; Matsumoto, T.; Nagatomo, S.; Tosha, T.; Terada, S.; Fujinami, S.; Suzuki, M.; Kitagawa, T. *J. Am. Chem. Soc.* **2005**, *127*, 5212–5223.
- (4) (a) Kitajima, N.; Hikichi, S.; Tanaka, M.; Moro-oka, Y. *J. Am. Chem. Soc.* **1993**, *115*, 5496–5508. (b) Company, A.; Jee, J.-E.; Ribas, X.; Lopez-Valbuena, J. M.; Gómez, L.; Corbella, M.; Llobet, A.; Mahía, J.; Benet-Buchholz, J.; Costas, M.; van Eldik, R. *Inorg. Chem.* **2007**, *46*, 9098–9110. (c) Lozano, A. A.; Sáez, M.; Pérez, J.; García, L.; Lezama, L.; Rojo, T.; López, G.; García, G.; Santana, M. D. *Dalton Trans.* **2006**, 3906–3911. (d) Ito, M.; Takita, Y. *Chem. Lett.* **1996**, 929–930.
- (5) Yoshimitsu, S.; Hikichi, S.; Akita, M. *Organometallics* **2002**, *21*, 3762–3773.
- (6) (a) Kitajima, N.; Fujisawa, K.; Moro-oka, Y.; Toriumi, K. *J. Am. Chem. Soc.* **1989**, *111*, 8976–8978. (b) Kitajima, N.; Fujisawa, K.; Fujimoto, C.; Moro-oka, Y.; Hashimoto, S.; Kitagawa, T.; Toriumi, K.; Tatsumi, K.; Nakamura, A. *J. Am. Chem. Soc.* **1992**, *114*, 1277–1291.
- (7) (a) Mahapatra, S.; Halfen, J. A.; Wilkinson, E. C.; Pan, G.; Wang, X.; Young, V. G., Jr.; Cramer, C. J.; Que, L., Jr.; Tolman, W. B. *J. Am. Chem. Soc.* **1996**, *118*, 11555–11574. (b) Mahapatra, S.; Halfen, J. A.; Tolman, W. B. *J. Am. Chem. Soc.* **1996**, *118*, 11575–11586.
- (8) (a) Do, L. H.; Lippard, S. J. *J. Am. Chem. Soc.* **2011**, *133*, 10568–10581. (b) Rinaldo, D.; Philipp, D. M.; Lippard, S. J.; Friesner, R. A. *J. Am. Chem. Soc.* **2007**, *129*, 3135–3147.
- (9) Xue, G.; Hont, R. D.; Münck, E.; Que, L., Jr. *Nat. Chem.* **2010**, *2*, 400–405.
- (10) Siegbahn, P. E. M.; Crabtree, R. H. *J. Am. Chem. Soc.* **1997**, *119*, 3103–3113.
- (11) Boudalis, A. K.; Clemente-Juan, J. M.; Dahan, F.; Psycharis, V.; Raptopoulos, C. P.; Donnadiu, B.; Sanakis, Y.; Tchuagues, J.-P. *Inorg. Chem.* **2008**, *47*, 11314–11323.
- (12) Avdeev, V. I.; Tapilin, V. M. *J. Phys. Chem. C* **2010**, *114*, 3609–3613.
- (13) Syn-linear core: Uehara, K.; Mizuno, N. *J. Am. Chem. Soc.* **2011**, *133*, 1622–1625.
- (14) (a) Ozerov, O. V. *Chem. Soc. Rev.* **2009**, *38*, 83–88. (b) Gokhate, A. A.; Dumesic, J. A.; Mavrikakis, M. *J. Am. Chem. Soc.* **2008**, *130*, 1402–1414. (c) Blum, O.; Milstein, D. *J. Am. Chem. Soc.* **2002**, *124*, 11456–11467.
- (15) (a) Bikondoa, O.; Pang, C. L.; Ithnin, R.; Muryan, C. A.; Onishi, H.; Thornton, G. *Nat. Mater.* **2006**, *5*, 189–192. (b) Shin, H.-J.; Jung, J.; Motobayashi, K.; Yanagisawa, S.; Morikawa, Y.; Kim, Y.; Kawai, M. *Nat. Mater.* **2010**, *9*, 442–447. (c) Oviedo, J.; Sánchez-de-Armas, R.; Miguel, M. S. A.; Sanz, J. F. *J. Phys. Chem. C* **2008**, *112*, 17737–17740. (d) Lindan, P. J. D.; Harrison, N. M.; Gillan, M. J. *Phys. Rev. Lett.* **1998**, *80*, 762–765.
- (16) (a) Menzel, D. *Science* **2002**, *295*, 58–59. (b) Feibelman, P. J. *Science* **2002**, *295*, 99–102. (c) Mitsui, T.; Rose, M. K.; Fomin, E.; Ogletree, D. F.; Salmeron, M. *Science* **2002**, *297*, 1850–1852. (d) Ludwig, R. *Angew. Chem., Int. Ed.* **2003**, *42*, 3458–3460. (e) Ogasawara, H.; Brena, B.; Nordlund, D.; Nyberg, M.; Pelmenchikov, A.; Pettersson, L. G. M.; Nilsson, A. *Phys. Rev. Lett.* **2002**, *89*, No. 276102. (f) Meyer, B.; Marx, D.; Dulub, O.; Diebold, U.; Kunat, M.; Langenberg, D.; Wöll, C. *Angew. Chem., Int. Ed.* **2004**, *43*, 6641–6645. (g) Wang, J. G.; Hammer, B. J. *J. Chem. Phys.* **2006**, *124*, No. 184704. (h) Coskuner, O.; Jarvis, E. A. A.; Allison, T. C. *Angew. Chem., Int. Ed.* **2007**, *46*, 7853–7855. (i) Tan, Q.-L.; Chen, Z.-X. *J. Chem. Phys.* **2007**, *127*, No. 104707. (j) Su, Z.; Bühl, M.; Zhou, W. *J. Am. Chem. Soc.* **2009**, *131*, 8697–8702.
- (17) (a) Wang, Y.; Nguyen, H. N.; Truong, T. N. *Chem.—Eur. J.* **2006**, *12*, 5859–5867. (b) Yin, S.; Ellis, D. E. *Surf. Sci.* **2008**, *602*, 2047–2054. (c) Ealet, B.; Goniakowski, J.; Finocchi, F. *Phys. Rev. B* **2004**, *69*, No. 195413.

- (18) (a) Thematic issues on polyoxometalate: Hill, C., Ed. *Chem. Rev.* **1998**, *98*, 1. (b) *Polyoxometalate Chemistry for Nano-Composite Design*; Yamase, T., Pope, M. T., Eds.; Kluwer: Dordrecht, The Netherlands, 2002. (c) Kozhevnikov, I. V., In *Catalysis by Polyoxometalates*, Wiley: Chichester, U.K., 2002. (d) Pope, M. T. In *Comprehensive Coordination Chemistry II*; Wedd, A. G., McCleverty, J. A., Meyer, T. J., Eds.; Elsevier: New York, 2004; Vol. 4, p 635. (e) Hill, C. L. In *Comprehensive Coordination Chemistry II*; Wedd, A. G., McCleverty, J. A., Meyer, T. J., Eds.; Elsevier: New York, 2004; Vol. 4, p 679. (f) Neumann, R. In *Modern Oxidation Methods*; Bäckvall, J. E., Ed.; Wiley-VCH: Weinheim, Germany, 2004; p 223. (g) Yu, R.; Kuang, X.-F.; Wu, X.-Y.; Lu, C.-Z.; Donahue, J. P. *Coord. Chem. Rev.* **2009**, *253*, 2872–2890.
- (19) Protic hydroxo complexes: (a) Nanthakumar, A.; Fox, S.; Murthy, N. N.; Karlin, K. D. *J. Am. Chem. Soc.* **1993**, *115*, 8513–8514. (b) Anandhi, U.; Sharp, P. R. *Inorg. Chem.* **2004**, *43*, 6780–6785. (c) Thorshang, K.; Fjeldahl, I.; Rømming, C.; Tilset, M. *Dalton Trans.* **2003**, 4051–4056.
- (20) (a) Kuznetsov, A. E.; Geletti, Y. V.; Hill, C. L.; Morokuma, K.; Musaev, D. G. *Theor. Chem. Acc.* **2011**, *130*, 197–207. (b) Wang, Y.; Zheng, G.; Morokuma, K.; Geletii, Y. V.; Hill, C. L.; Musaev, D. G. *J. Phys. Chem. B* **2006**, *110*, 5230–5237. (c) Quiñero, D. Q.; Wang, Y.; Morokuma, K.; Kharvutskii, L. A.; Botar, B.; Geletii, Y. V.; Hill, C. L.; Musaev, D. G. *J. Phys. Chem. B* **2006**, *110*, 170–173. (d) Musaev, D.; Morokuma, K.; Geletii, Y. V.; Hill, C. L. *Inorg. Chem.* **2004**, *43*, 7702–7708.
- (21) (a) Mbomekallé, I.-M.; López, X.; Poblet, J. M.; Sécheresse, F.; Keita, B.; Nadjó, L. *Inorg. Chem.* **2010**, *49*, 7001–7006. (b) Poblet, J. M.; López, X.; Bo, C. *Chem. Soc. Rev.* **2003**, *32*, 297–308.
- (22) Brese, N. E.; O’Keeffe, M. *Acta Crystallogr.* **1991**, *B47*, 192–197.
- (23) (a) Wieghardt, K.; Bossek, U.; Volckmar, K.; Swiridoff, W.; Weiss, J. *Inorg. Chem.* **1984**, *23*, 1387–1389. (b) Neves, A.; Wieghardt, K.; Nuber, B.; Weiss, J. *Inorg. Chim. Acta* **1988**, *150*, 183–187.
- (24) Anti-linear core: (a) Ghosh, S.; Nanda, K. K.; Addison, A. W.; Butcher, R. J. *Inorg. Chem.* **2002**, *41*, 2243–2249. (b) Holwerda, R. A.; Whittlesey, B. R.; Nilges, M. J. *Inorg. Chem.* **1998**, *37*, 64–68. (c) Yamada, S.; Katayama, C.; Tanaka, J.; Tanaka, M. *Inorg. Chem.* **1984**, *23*, 253–255. (d) Launay, J.-P.; Jeannin, Y.; Daoudi, M. *Inorg. Chem.* **1985**, *24*, 1052–1059. (e) Toftlund, H.; Larsen, S.; Murray, K. S. *Inorg. Chem.* **1991**, *30*, 3964–3967.
- (25) Anti-angular core: (a) Bellemin-Lapponnaz, S.; Coleman, K. S.; Dierkes, P.; Masson, J.-P.; Osborn, J. A. *Eur. J. Inorg. Chem.* **2000**, 1645–1649. (b) Hoppe, E.; Limberg, C.; Ziemer, B. *Inorg. Chem.* **2006**, *45*, 8308–8317. (c) Chatterjee, P. J.; Bhattacharya, S.; Audhya, A.; Choi, K.-Y.; Endo, A.; Chaudhury, M. *Inorg. Chem.* **2008**, *47*, 4891–4902. (d) Nielsen, K.; Fehrmann, R.; Eriksen, K. M. *Inorg. Chem.* **1993**, *32*, 4825–4828. (e) Chakravarty, J.; Dutta, S.; Chakravorty, A. *J. Chem. Soc., Dalton Trans.* **1993**, 2857–2858. (f) Schulz, D.; Weyhermüller, T.; Wieghardt, K.; Nuber, B. *Inorg. Chim. Acta* **1995**, *240*, 217–229.
- (26) Twist-linear core: (a) Rowan, M. A.; Warford, L.; Homden, D. M.; Arbaoui, A.; Elsegood, M. R.; Dale, S. H.; Yamato, T.; Casas, C. P.; Matsui, S.; Matsuura, S. *Chem.—Eur. J.* **2007**, *13*, 1090–1107. (b) Yamada, S.; Katayama, C.; Tanaka, J.; Tanaka, M. *Inorg. Chem.* **1984**, *23*, 253–255. (c) Dinda, R.; Sengupta, P.; Ghosh, S.; Mak, T. C. W. *Inorg. Chem.* **2002**, *41*, 1684–1688. (d) Sangeetha, N. R.; Pal, S. *Bull. Chem. Soc. Jpn.* **2000**, *73*, 357–363. (e) Pessoa, J. C.; Silva, A. L.; Vieira, A. L.; Vilas-Boas, L.; O’Brien, P. O. *J. Chem. Soc., Dalton Trans.* **1992**, 1745–1749. (f) Dutta, S. K.; Kumar, S. B.; Bhattacharyya, S.; Tiekink, E. R. T.; Chaudhury, M. *Inorg. Chem.* **1997**, *36*, 4954–4960. (g) Dutta, S. K.; Samanta, S.; Kumar, S. B.; Han, O. H.; Burckel, P.; Pinkerton, A. A.; Chaudhury, M. *Inorg. Chem.* **1999**, *38*, 1982–1988.
- (27) Twist-angular core: (a) Dutta, S.; Basu, P.; Chakravorty, A. *Inorg. Chem.* **1993**, *32*, 5343–5348. (b) Dai, J.; Akiyama, S.; Munakata, M.; Mikuriya, M. *Polyhedron* **1994**, *13*, 2495–2499. (c) Grüning, C.; Schmidt, H.; Rehder, D. *Inorg. Chem. Commun.* **1999**, 57–59. (d) Schmidt, H.; Bashirpoor, M.; Rehder, D. *J. Chem. Soc., Dalton Trans.* **1996**, 3865–3870. (e) Vigato, U. C. P. A.; Graziani, R.; Vidali, M.; Milani, F.; Musiani, M. M. *Inorg. Chim. Acta* **1982**, *61*, 121–128.
- (f) Ludwig, E.; Hefele, H.; Schilde, U.; Uhlemann, E. Z. *Anorg. Allg. Chem.* **1994**, *620*, 346–352. (g) Mondal, S.; Ghosh, P.; Chakravorty, A. *Inorg. Chem.* **1997**, *36*, 59–63. (h) Chatterjee, P. B.; Kundu, N.; Bhattacharya, S.; Choi, K.-Y.; Endo, A.; Chaudhury, M. *Inorg. Chem.* **2007**, *46*, 5483–5485. (i) Wang, D.; Behrens, A.; Farahbakhsh, M.; Gärtens, J.; Rehder, D. *Chem.—Eur. J.* **2003**, *9*, 1805–1813.
- (28) Syn-angular core: Knopp, P.; Wieghardt, K.; Nuber, B.; Weiss, J.; Sheldrick, W. S. *Inorg. Chem.* **1990**, *29*, 363–371.
- (29) Frisch, M. J.; et al. *Gaussian09, Revision B.01*; Gaussian, Inc., Wallingford, CT, 2009.
- (30) Tomasi, J.; Mennucci, B.; Cammi, R. *Chem. Rev.* **2005**, *105*, 2999–3094.
- (31) Molekel 5.4 is the molecular visualization program developed by the visualization group at the Swiss national supercomputing center (CSCS).
- (32) As is also the case with 2^{Si} [HOMO–4 (242) and HOMO–5 (241) orbitals], the oxo-deficient V–O–V core in 2^{Ge} was stabilized by weak d_{π} – p_{π} – d_{π} interactions represented by HOMO–4 (253) and HOMO–5 (252) orbitals (Figure 3). The reason why the V–O–V unit was bent toward $[\gamma\text{-GeW}_{10}\text{O}_{36}]^{8-}$ is formation of the hybrid orbital among O(113) bridging oxo ligand and O(136) and O(137) in a GeO_4 unit represented by HOMO–6 (251). Similar results were obtained by calculations under vacuum conditions (Figure S4, Supporting Information).
- (33) Ho, J.; Coote, M. L. *Theor. Chem. Acc.* **2010**, *125*, 3–21.
- (34) Nsouli, N. H.; Bassil, B. M.; Dickman, M. H.; Kortz, U.; Keita, B.; Nadjó, L. *Inorg. Chem.* **2006**, *45*, 3858–3860.
- (35) *International Tables for X-ray Crystallography*; Kynoch Press: Birmingham, U.K., 1975; Vol. 4.
- (36) Otwinowski, Z.; Minor, W. Processing of X-ray Diffraction Data Collected in Oscillation Mode. In *Methods in Enzymology, Macromolecular Crystallography, Part A*; Carter, C. W., Jr., Sweet, R. M., Eds.; Academic Press: New York, 1997; Vol. 276, p 307.
- (37) Sheldrick, G. M. *SHELX-97, Programs for Crystal Structure Analysis*, release 97-2; University of Göttingen: Göttingen, Germany, 1997.
- (38) Farrugia, L. J. *J. Appl. Crystallogr.* **1999**, *32*, 837–838.